Available online at www.sciencedirect.com
SCIENCE DIRECT®
International Journal of Heat and Mass Transfer 48 (2005) 2452–2463
International Journal of HEAT and MASS TRANSFER
www.elsevier.com/locate/ijhmt

Natural convection in metal foams with open cells

C.Y. Zhao [a,b,*], T.J. Lu [c,d], H.P. Hodson [c]

[a] State Key Laboratory of Multiphase Flow, School of Energy and Power Engineering, Xi'an Jiaotong University, Shaanxi 710049, P.R. China
[b] Department of Mechanical Engineering, School of Engineering and Design, Brunel University, Uxbridge UB8 3PH, UK
[c] Department of Engineering, University of Cambridge, Trumpington Street, Cambridge CB2 1PZ, UK
[d] School of Aeronautics and Astronautics, Xi'an Jiaotong University. Shaanxi 710049, P.R. China

Received 29 March 2004; received in revised form 3 December 2004
Available online 13 March 2005

Abstract

This paper presents a combined experimental and numerical study on natural convection in open-celled metal foams. The effective thermal conductivities of steel alloy (FeCrAlY) samples with different relative densities and cell sizes are measured with the guarded-hot-plate method. To examine the natural convection effect, the measurements are conducted under both vacuum and ambient conditions for a range of temperatures. The experimental results show that natural convection is very significant, accounting for up to 50% of the effective foam conductivity obtained at ambient pressure. This has been attributed to the high porosity ($\varepsilon > 0.9$) and inter-connected open cells of the metal foams studied.

Morphological parameters characterizing open-celled FeCrAlY foams are subsequently identified and their cross-relationships are built. The non-equilibrium two-equation energy transfer model is employed, and selected calculations show that the non-equilibrium effect between the solid foam skeleton and air is significant. The study indicates that the combined parameter, i.e., the porous medium Rayleigh number, is no longer appropriate to correlate natural convection by itself when the Darcy number is sufficiently large as in the case of natural convection in open-celled metal foams. Good agreement between model predictions and experimental measurements is obtained.

Keywords: Cellular metal foams; Natural convection; Thermal conductivity; Modeling; Measurements

1. Introduction

Natural convection in porous media has been extensively investigated due to the wide range of applications in geothermal systems, electronics cooling, crude oil production, storage of nuclear waste materials, fiber and granular insulations, solidification of castings, amongst many others. Most of previous studies [1–14] have focused on natural convection in packed beds and granular porous media with porosities in the range 0.3–0.5. The porosity of a typical metal foam with open cells is usually much higher ($\varepsilon > 0.9$), and the ligaments form a network of inter-connected dodecahedral-like cells, as shown in Fig. 1a. Consequently, most of previous studies are not applicable to highly porous, open-celled metal foams, and it is expected that the effect

* Corresponding author. Tel.: +44 1895 266697; fax: +44 1895 256392.
E-mail addresses: chang-ying.zhao@brunel.ac.uk, cyzhao@mail.xjtu.edu.cn (C.Y. Zhao).

0017-9310/$ - see front matter © 2005 Elsevier Ltd. All rights reserved.
doi:10.1016/j.ijheatmasstransfer.2005.01.002

Nomenclature

$\tilde{a}$	surface area density, 1/m
C_f	specific heat of fluid, J/kg K
C_I	inertial constant
d_p	cell size, m
d_f	cell ligament diameter, m
Da	Darcy number = K/H^2
g	gravitational acceleration, m/s^2
H	specimen height, m
k	thermal conductivity, W/mK
k_m	saturated medium thermal conductivity, W/mK
k_d	dispersion conductivity, W/mK
K	permeability, W/mK
Nu	Nusselt number
P	pressure, Pa
Pr	Prandtl number = ν_f/α_f
Ra	Rayleigh number = $g\beta\Delta TH^3/(\nu_f/\alpha_f)$
Ra_m	medium Rayleigh number = $RaDak_f/k_m$
T	temperature, K
u	x-component velocity, m/s
v	r-component velocity, m/s
U	dimensionless x-component velocity
V	dimensionless x-component velocity

Greek symbols

α	thermal diffusivity, m^2/s
β	coefficient of thermal expansion, K^{-1}
ε	porosity
θ	dimensionless temperature = $(T - T_c)/(T_h - T_c)$
μ	dynamic viscosity, Ns/m^2
ν	kinematic viscosity, m^2/s
ρ	fluid density, kg/m^3

Subscripts

c	cold
d	dispersion
h	hot
e	effective
f	fluid
m	medium
s	solid

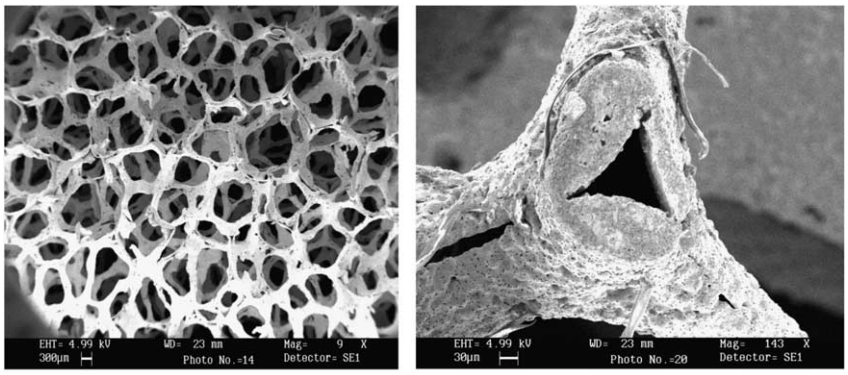

Fig. 1. A typical Porvair FeCrAlY foam: (a) cellular morphology; (b) cross-section of an individual strut.

of natural convection in these foams could be much stronger than that in packed beds and granular porous media.

To the authors' best knowledge, in the open literatures, Hong et al. [15] analytically studied the natural convection boundary layer from a heated vertical plate embedded in a metal foam by using the single perturbation method. It was concluded that although non-Darcy effects, i.e., boundary and inertial effects, are very significant in metal foams, they are not important in low-porosity media such as packed beds. However, in this study [15] the microstructure of a metal foam was not really introduced, rather it was explored by simply changing relevant parameters such as Rayleigh number and Prandtl number. Recently Phanikumar and Mahajan [16] studied the natural convection in an enclosure in which a metal foam occupies one corner of the enclosure. In this paper, the flow and temperature fields in the enclosure are examined, but the details of flow pattern and temperature distribution in metal foams are not revealed. Consequently, natural convection in metal foams needs to be further studied by modeling the parameters in terms of mircostructural parameters. In addition, almost all previous studies for packed beds employed

the one-equation energy model based upon the assumption that local thermal equilibrium between fluid and solid phases is achieved. However, there exists no concrete evidence to justify this assumption. For metal foams where the solid conductivity is much lager than that of air, it is expected the temperature distributions are significantly different for the solid and fluid. Therefore the non-equilibrium effect needs to be examined based on the two-equation model. Furthermore, in previous studies, the entry region is usually quite short so that the convective term in the governing equations can be neglected. This may not be the case for natural convection in high-porosity metal foams.

In all previous studies on natural convection, the permeability K is derived from forced convection experiments. The permeability and inertial constant C_I of a metal foam have been investigated by several researchers [17–20], although only Calmidi and Mahajan [19], gave specific formulations of K and C_I based on experimental measurements at high velocity range, e.g., 0.5–7 m/s. However, the velocity of natural convection in metal foams is several orders of magnitude smaller. Some studies [21–23] have shown that K and C_I are both velocity dependent, because linear and quadratic effects on pressure loss are always present. Depending on the velocity range one effect will be stronger (or weaker) than the other, and this will be reflected in the value of the coefficients for the linear and quadratic terms. Therefore, it is important that K and C_I are associated with the velocity range from which they are determined. In other words, these values of K and C_I cannot be used with confidence for predicting hydraulic behaviour at velocities outside this range.

Hitherto no experimental data is available for open-celled metal foams to give a clear indication on how important natural convection is, what percentage it can contribute to overall effective thermal conductivity, and how its effect changes with increasing temperature (in which case the viscosity increases and thermal radiation effect becomes significant). All these questions need to be experimentally and analytically/numerically addressed.

The objective of this paper is multifold. The effect of natural convection on the effective thermal conductivity of open-celled metal foams will be experimentally determined. The mathematical formulations based on the non-equilibrium two energy equation model will be normalized, and the independent parameters charactering natural convection will be identified. The Rayleigh number and Darcy number effects will be examined and non-equilibrium effect will be revealed. The predictions will be compared with experimental measurements at room temperature. Natural convection in metal foams at high temperatures is beyond the scope of the present paper, and will be addressed in combination with thermal radiation effect in a separate study.

2. Experimental program

2.1. Apparatus

The guarded-hot-plate apparatus in the one-sided mode, based on ASTM C1044-90 and C177, is used for thermal conductivity measurements. The principle is to ensure a unidirectional heat flux between the top and bottom surfaces of the specimen. Detailed descriptions of the apparatus have been given by Zhao et al. [24], and hence, for brevity, only the general arrangement of the measurement is given below.

A successful guarded-hot-plate apparatus enabling measurement at varying temperatures and air pressures requires a complex system. The experimental apparatus consists of a test section and various supporting systems, as shown in Fig. 2. The test section contains main heater, auxiliary heaters, specimen, cooling plate, thermal insulations, and thermocouples. It is located in a vacuum chamber, being part of the vacuum system, and enables experiments to be carried out at various air pressures. The electric power to the heaters is supplied by a heater control system. The cold plate temperature can be varied by adjusting the amount of air flow through the system. Thermocouple signals and the power input to the main heater are recorded and analysed by a data logging system.

2.2. Experimental uncertainty analysis

The uncertainty of the measured results is caused by random as well as systematic errors in the measurements, mainly consisting of:

- Uncertainty in heat flow, δQ.
- Uncertainty in temperature difference, $\delta\Delta T = \delta(T_h - T_c)$.
- Uncertainty in metered area, δA.
- Uncertainty in specimen thickness, δH.

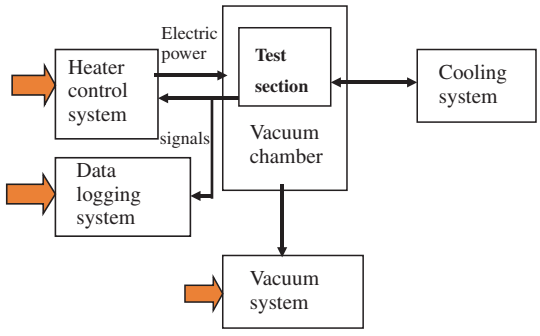

Fig. 2. General arrangement of the test facility.

The total uncertainty of the measurement can be obtained as:

$$\frac{\delta k_e}{k_e} = \sqrt{\left(\frac{\delta Q}{Q}\right)^2 + \left(\frac{\delta \Delta T}{\Delta T}\right)^2 + \left(\frac{\delta A}{A}\right)^2 + \left(\frac{\delta H}{H}\right)^2} \quad (1)$$

The above four uncertainties have been individually analysed by Zhao et al. [24]. Generally, the uncertainty of the present measurement lies within the range between 5% and 8%.

2.3. Experimental results

A total of five FeCrAlY (Fe 73%, Cr 20%, Al 5%, Y 2%) foam disks of roughly 25 mm thickness and 100 mm diameter, with a range of pore sizes and relative densities, were produced via the sintering route and supplied by Porvair Fuel Cell Technology. Their relative densities and cell sizes expressed in terms of ppi (pores per inch) are given in Table 1. In the measurements, the hot plate temperature is maintained at about 40 °C, whilst the temperature difference between hot and cold plates is kept at approximately $\Delta T = 20$ °C. The effective thermal conductivity of the foam is calculated according to $k_e = qH/\Delta T$, where q is the input heat flux and H is the specimen height. More details of the measurement procedures can be found in the paper [24].

Fig. 3 presents the measured results for all five samples under both vacuum condition and atmospherific pressure. It can be seen that the value of k_e at atmospherific pressure is roughly twice that in vacuum. This clearly indicates that the effect of natural convection is very significant, contributing about 50% of the overall thermal conductivity measured at atmospherific pressure. The main reason is that the porosity of metal foams is very high, usually over 90%, and the cells are open and inter-connected. Natural convection therefore takes place in the global domain, rather than occurring inside a single cell.

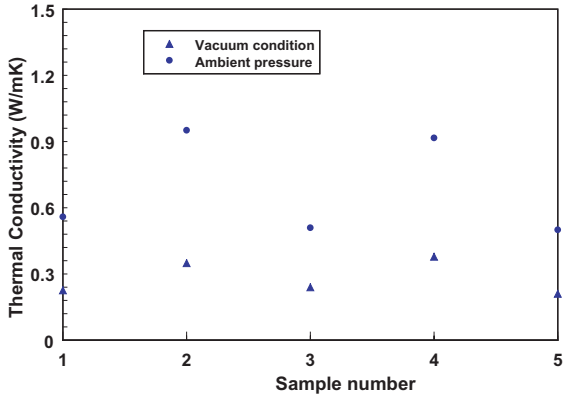

Fig. 3. Experimental results at both vacuum condition and ambient pressure.

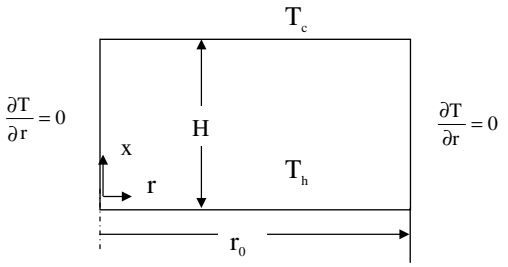

Fig. 4. Physical model and cylindrical coordinate system.

3. Theoretical simulation

3.1. Mathematical formulations

For the two-dimensional axisymmetric, steady state, natural convection studied in the present paper, the physical model is depicted in Fig. 4. The bottom and top surfaces of the specimen are maintained at uniform temperatures, T_h and T_c, respectively, with $T_h > T_c$. The side walls are thermally insulated. The problem under investigation is natural convection of incompressible fluid flow through open-celled metal foams, belonging to the general class of porous Rayleigh-Benard problem.

When the temperature difference $T_h - T_c$, characterized by the dimensionless parameter Rayleigh number Ra, is not too high, heat is transported mainly by conduction. However, when the Rayleigh number exceeds a certain critical value Ra_c, the colder and denser fluid at the top tends to topple over. The fluid becomes unstable and two-dimensional cellular patterns appear. It is believed that increasing the Rayleigh number further results in three-dimensional cellular patterns and eventually chaotic motion, which is difficult to model physically. As previously discussed, the complexity of the morphological structure of a porous medium usually precludes a detailed microscopic investigation of transport phenomena at the pore level. Therefore, the general

Table 1
Specifications of FeCrAlY samples tested

	Sample 1	Sample 2	Sample 3	Sample 4	Sample 5
PPI (pores per inch)	30	30	60	60	90
Relative density	5%	10%	5%	10%	5%

transport equations are commonly integrated over a representative elementary volume, accommodating both the fluid and solid phases within a porous structure.

There are two approaches available in applying the volume-averaging technique for heat transfer investigations: one is averaging over a representative elementary volume containing both the fluid and the solid phases, and the other is averaging separately over each of the phases, thus resulting in a separate energy equation for each individual phase. These two models are referred to as the one-equation model and two-equation model, respectively. The one-equation model is valid when local temperature difference between fluid and solid phases is negligibly small. Because this temperature difference cannot in general be neglected in metal foams saturated with air [19,25,26], the two-equation model will be used below.

Throughout this study, the thermophysical properties of air are assumed constant, except for its density contained in the momentum equation. To an excellent approximation, the metal foam can be considered homogeneous and isotropic. In order to re-examine the momentum equation through a highly porous medium, the boundary and inertial effects are included with volume-averaging principles. Under these conditions, the governing equations are given by:

Continuity equation

$$\nabla \cdot \langle \mathbf{V} \rangle = 0 \tag{2}$$

Momentum equation

$$\frac{\rho_f}{\varepsilon^2}\langle(\mathbf{V}\cdot\nabla)\mathbf{V}\rangle = -\nabla\langle P\rangle_f + \frac{\mu_f}{\varepsilon}\nabla^2\langle\mathbf{V}\rangle - \frac{\mu_f}{K}\langle\mathbf{V}\rangle - \rho_f\frac{C_I}{\sqrt{K}}[\langle\mathbf{V}\rangle\cdot\langle\mathbf{V}\rangle]J + \rho_f g_i \tag{3}$$

The fourth term in Eq. (3) was first introduced by Forchheimer to account for the inertial effects (non-Darcy flow). Similarly, the second term in (3) accounts for the boundary effects on velocity distribution, and was first introduced by Brinkman. The last term in (3) is the buoyancy term, i.e., the gravity vector, which is the driving force behind natural convection.

Solid phase energy equation

$$0 = \nabla\cdot\{k_{se}\cdot\nabla\langle T_s\rangle\} - h_{sf}\tilde{a}(\langle T_s\rangle - \langle T_f\rangle) \tag{4}$$

Fluid phase energy equation

$$\langle\rho\rangle_f C_f\langle\mathbf{V}\rangle\cdot\nabla\langle T_f\rangle = \nabla\cdot\{(k_{fe}+k_d)\cdot\nabla\langle T_f\rangle\} + h_{sf}\tilde{a}(\langle T_s\rangle - \langle T_f\rangle) \tag{5}$$

where $\langle\,\rangle$ means a volume-averaging; k_{se}, T, h_{sf}, $\tilde{a}$, ρ_f, μ_f, C_f and k_{fe} are effective solid thermal conductivity, temperature, interfacial heat transfer coefficient, wetted area per volume, density, viscosity, heat capacity and effective fluid thermal conductivity, respectively; k_d is thermal dispersion conductivity (its physical significance and formulation will be given later), ε is porosity, $\mathbf{V}$ is velocity vector, and $J = \mathbf{V}_p/|\mathbf{V}_p|$ is unit vector aligned along pore velocity vector, $\mathbf{V}_p$; K is permeability of the porous medium with unit m^2, and it will be re-examined for buoyancy-driven natural convection later. C_I is the inertial coefficient, depending on the porous microstructure.

For low-porosity media such as packed beds, the convective term $\frac{\rho_f}{\varepsilon^2}\langle(\mathbf{V}\cdot\nabla)\mathbf{V}\rangle$ in (3) is usually very small and can be neglected. For high-porosity media such as metal foams, convective effects may nevertheless be important and hence this term will be reserved in the present study. Although Hong et al. [15] concluded that the effect of inertial term in Eq. (3) is significant by simply changing the inertial coefficient, no experimental validation was given in their study. In the present study, the inertial term—the fourth term will not be considered owing to the small velocity and the lack of reliable correlation for C_I. Due to small variations in fluid density, the Boussinesq approximation will be invoked to allow for density variations in the buoyancy term of Eq. (3), while fluid density remains constant for all other terms. By splitting the velocity vector into two components, u in the x-direction and v in the r-direction, Eqs. (3)–(5) can be re-arranged and simplified as follows:

Momentum equations

$$\frac{\partial(\rho_f u^2)}{\partial x} + \frac{1}{r}\frac{\partial(r\rho_f uv)}{\partial r} = -\varepsilon^2\frac{\partial p}{\partial x} + \frac{\partial}{\partial x}\left(\mu_f\varepsilon\frac{\partial u}{\partial x}\right) + \frac{1}{r}\frac{\partial}{\partial r}\left(r\mu_f\varepsilon\frac{\partial u}{\partial r}\right) - \frac{\mu_f\varepsilon^2}{K}u + \rho_f g\beta(T_f - T_c)\varepsilon^2 \tag{6}$$

$$\frac{\partial(\rho_f uv)}{\partial x} + \frac{1}{r}\frac{\partial(r\rho_f v^2)}{\partial r} = -\varepsilon^2\frac{\partial p}{\partial r} + \frac{\partial}{\partial x}\left(\mu_f\varepsilon\frac{\partial v}{\partial x}\right) + \frac{1}{r}\frac{\partial}{\partial r}\left(r\mu_f\varepsilon\frac{\partial v}{\partial r}\right) - \frac{\mu_f\varepsilon^2}{K}v \tag{7}$$

where β is the thermal expansion coefficient of the fluid, and g is gravitational acceleration.

Energy equations

$$0 = \frac{\partial}{\partial x}\left(k_{se}\frac{\partial T_s}{\partial x}\right) + \frac{1}{r}\frac{\partial}{\partial r}\left(rk_{se}\frac{\partial T_s}{\partial r}\right) - h_{sf}\tilde{a}(T_s - T_f) \tag{8}$$

$$\frac{\partial(\rho_f uT_f)}{\partial x} + \frac{1}{r}\frac{\partial(rvT_f)}{\partial r} = \frac{\partial}{\partial x}\left(\frac{k_{fe}+k_d}{C_f}\frac{\partial T_f}{\partial x}\right) + \frac{1}{r}\frac{\partial}{\partial r}\left(r\frac{k_{fe}+k_d}{C_f}\frac{\partial T_f}{\partial r}\right) + \frac{\tilde{a}h_s}{C_f}(T_s - T_f) \tag{9}$$

The governing equations (6)–(9) are subject to the following boundary conditions:

$$
\begin{aligned}
&u = v = 0 \quad \text{and} \quad T_s = T_f = T_h \quad \text{at } x = 0\\
&u = v = 0 \quad \text{and} \quad T_s = T_f = T_c \quad \text{at } x = H\\
&v = 0 \ \frac{\partial u}{\partial r} = 0 \quad \text{and} \quad \frac{\partial T_s}{\partial r} = \frac{\partial T_f}{\partial r} = 0 \quad \text{at } r = 0\\
&u = v = 0 \quad \text{and} \quad \frac{\partial T_s}{\partial r} = \frac{\partial T_f}{\partial r} = 0 \quad \text{at } r = r_0
\end{aligned}
\tag{10}
$$

where H and r_0 are the height and radius of the cylindrical specimen, respectively.

3.2. Normalization of governing equations

In order to identify the important parameters characterizing natural convection in metal foams and to have a clear understanding of the physical problem, normalization of the above governing equations is necessary. Upon introducing the following non-dimensional quantities:

$$
X = \frac{x}{H}, \quad R = \frac{r}{H}, \quad U = \frac{uH}{\alpha_f}, \quad V = \frac{vH}{\alpha_f}, \quad \theta = \frac{T - T_c}{T_h - T_c} \tag{11}
$$

where $\alpha_f = k_f/(\rho_f C_f)$ is the air thermal diffusivity, the governing equations (6)–(9) can be non-dimensionalized, as:

Momentum equations

$$
\begin{aligned}
&\frac{\partial U^2}{\partial X} + \frac{1}{R}\frac{\partial (RUV)}{\partial R}\\
&\quad = -\frac{\partial P}{\partial X} + \frac{\partial}{\partial X}\left(P_r \varepsilon \frac{\partial U}{\partial X}\right) + \frac{1}{R}\frac{\partial}{\partial R}\left(RP_r \varepsilon \frac{\partial U}{\partial R}\right)\\
&\qquad - \frac{\varepsilon^2 P_r}{Da} U + R_a P_r \theta_f \varepsilon^2
\end{aligned}
\tag{12}
$$

$$
\begin{aligned}
&\frac{\partial (UV)}{\partial X} + \frac{1}{R}\frac{\partial (RV^2)}{\partial R}\\
&\quad = -\frac{\partial P}{\partial R} + \frac{\partial}{\partial X}\left(P_r \varepsilon \frac{\partial V}{\partial X}\right) + \frac{1}{R}\frac{\partial}{\partial R}\left(RP_r \varepsilon \frac{\partial V}{\partial R}\right) - \frac{\varepsilon^2 P_r}{Da} V
\end{aligned}
\tag{13}
$$

$$
\frac{\partial}{\partial X}\left(\frac{\partial \theta_s}{\partial X}\right) + \frac{1}{R}\frac{\partial}{\partial R}\left(R\frac{\partial \theta_s}{\partial R}\right) - B_{ioe}(\theta_s - \theta_f) = 0 \tag{14}
$$

$$
\begin{aligned}
&\frac{\partial (U\theta_f)}{\partial X} + \frac{1}{R}\frac{(RV\theta_f)}{\partial R}\\
&\quad = \frac{\partial}{\partial X}\left(\frac{\alpha_{fe} + \alpha_d}{\alpha_f}\frac{\partial \theta_f}{\partial X}\right) + \frac{1}{R}\frac{\partial}{\partial R}\left(R\frac{\alpha_{fe} + \alpha_d}{\alpha_f}\frac{\partial \theta_f}{\partial R}\right) + Nu_i\\
&\quad = 0
\end{aligned}
\tag{15}
$$

It is noted that a total of five parameters appear in the governing equations, namely, Darcy number (Da), Rayleigh number (Ra), interfacial Biot number (B_{ioe}), interfacial Nusselt number (Nu_i), and equivalent fluid diffusivity ratio:

$$
\begin{aligned}
&Da = \frac{K}{H^2}, \quad Ra = \frac{g\beta \Delta T H^3}{a_f \nu_f}, \quad B_{ioe} = \frac{\tilde{a} H^2 h_i}{k_{se}},\\
&Nu_i = \frac{\tilde{a} H^2 h_i}{k_f}, \quad \frac{\alpha_{fe} + \alpha_d}{\alpha_f} = \frac{k_{fe} + k_d}{k_f}
\end{aligned}
\tag{16}
$$

3.3. Modelling on Porvair metal foams

3.3.1. Independent parameters

The relative density ρ_r, pore size d_p, ligament diameter d_f, and inner-to-outer ligament diameter ratio r have already been experimentally measured [25,26]. These parameters are not all independent of each other, and the cross-relationship can be written as [19]:

$$
\frac{d_f}{d_p} = 1.18\sqrt{\frac{1-\varepsilon}{3\pi}}\left(\frac{1}{1 - e^{-((1-\varepsilon)/0.04)}}\right) \tag{17}
$$

It should be pointed out that Eq. (17) has been shown to adequately describe the cellular morphology of ERG foams for which the simple relation between porosity and relative density holds, $\rho_r = 1 - \varepsilon$. Thus, for ERG foams, there are only two independent foam parameters, i.e., pore size d_p (or fibre diameter d_f), and porosity ε (or relative density ρ_r).

For *Porvair* metal foams, because cell edge ligaments are hollow (Fig. 1b), another parameter, the inner-to-outer ligament diameter ratio r, is needed. The relationship between porosity and relative density then becomes:

$$
\rho_r = (1 - \varepsilon)(1 - r^2) \tag{18}
$$

Consequently, the following cross-relationships exist between a ERG foam and a *Porvair* foam:

$$
\rho_{r,Porvair} = \rho_{r,ERG}(1 - r^2) \quad \text{at same porosity } \varepsilon \tag{19}
$$

$$
\varepsilon_{porvair} = \frac{\varepsilon_{ERG} - r^2}{1 - r^2} \quad \text{at same relative density } \rho_r \tag{20}
$$

From Eqs. (17)–(20), it can be seen that there are three independent parameters characterizing a Porvair foam, namely, porosity ε (or relative density ρ_r), pore size d_p (or ligament diameter d_f), and inner-to-outer ligament diameter ratio r. From Eq. (18), it is noted that the relative density and inner-to-outer ligament diameter ratio can be integrated into one parameter, i.e., the porosity. Consequently, similar to the case of a ERG foam, there are only two independent parameters for a Porvair foam, i.e., porosity and pore size (or ligament diameter). The comparison between predictions and measured morphology data for Porvair foams was given by Zhao et al. [26].

3.3.2. Permeability K

The concept of permeability K was first introduced by Darcy to build the relationship between pressure gradient and area-averaged fluid velocity through a column of porous material [27]. With reference to one-dimensional forced flow by pressure gradient, the Darcy law is:

$$u = \frac{K}{\mu}\left(-\frac{\mathrm{d}p}{\mathrm{d}x}\right) \tag{21}$$

from which the permeability can be expressed as

$$K = \frac{\mu u}{-\mathrm{d}p/\mathrm{d}x} = (\text{length})^2 \tag{22}$$

The concept of permeability K has been widely used to describe laminar flow driven by pressure gradient in a porous medium, with the square root of K representing a length scale of the velocity field. The length scale of buoyancy-driven natural convection should be quite different, because the flow pattern and velocity range are quite different in the two physically different problems. This situation is similar to the case of buoyancy turbulence, wherein the buoyancy turbulence length scale is different from that associated with the turbulence driven by shear force. In other words, K obtained from forced convection measurement is not adequate for natural convection due to different velocity range and flow pattern.

The above discussions suggest that permeability K is a much complicated parameter. The theoretical determination of K for the velocity range of natural convection in metal foams is not applicable due to the lack of experimental data. Rather, the Da ($=K/H^2$) effect will first be examined, from which it will be shown, fortunately, that heat transfer will gradually reach a plateau after Da exceeds a certain value for a fixed specimen height and Rayleigh number, Ra. In view of the high porosity (>90%) and inter-connected open cells of metal foams, it is assumed that the Da number lies in the plateau region for the five FeCrAlY samples tested. This implies that the foam structure imposes little restriction on natural convection flow at the global scale, with its velocity determined mainly by Ra, consistent with the global nature of natural convection in metal foams.

3.3.3. Effective thermal conductivity

The effective solid and fluid conductivities, k_{se} and k_{fe}, appearing in Eqs. (8) and (9) need to be determined in order to close the equations. A three-dimensional analytical model for the effective conductivity of open-celled metal foams having solid struts (e.g., ERG foams) has recently been put forward by Boomsma and Poulikakos [28]. With thermal radiation and air conduction neglected, this model yields:

$$\frac{k_{se}}{k_s} = \frac{1}{\sqrt{2}}\left\{\frac{4\lambda}{2e^2+\pi\lambda(1-e)} + \frac{3e-2\lambda}{e^2} + \frac{\left(\sqrt{2}-2e\right)^2}{2\pi\lambda^2\left(1-2e\sqrt{2}\right)}\right\}^{-1} \tag{23}$$

where $e = 0.339$,

$$\lambda = \sqrt{\frac{\sqrt{2}\left(2-(5/8)e^3\sqrt{2}-2\varepsilon\right)}{\pi\left(3-4e\sqrt{2}-e\right)}} \tag{24}$$

and ε is the porosity of the foam having solid cell ligaments. Porvair foams have similar cellular morphologies as ERG foams except that their cell ligaments are typically hollow, and hence the porosity and effective solid conductivity need to be changed accordingly [26]. If the Porvair foam has the same relative density as the ERG material, then its porosity can be calculated according to:

$$\varepsilon_{\text{porvair}} = \frac{\varepsilon - r^2}{1 - r^2} \tag{25}$$

where r is the inner-to-outer radius ratio of the hollow struts in Porvair foams [26]; see also Fig. 1b. Similarly, the effective solid conductivity of a Porvair foam is calculated as

$$k_{\text{se,porvair}} = k_{\text{se}}(1-r)^2 \tag{26}$$

where k_{se} is the value obtained from Eq. (23).

3.3.4. Thermal dispersion conductivity k_d

Thermal dispersion in a fluid-saturated porous medium represents the enhancement of heat transfer due to hydrodynamic mixing of interstitial fluid at the pore scale. Fluid particles, flowing along separate paths inside a metal foam will be pushed apart when they meet cell ligaments, and thus dispersed by these solid obstructions, leading to enhanced mixing. This is the physical rational behind the so-called thermal dispersion conductivity k_d. Therefore the macroscopic concept of thermal dispersion stems from local temperature and velocity deviations. Although the net effect is macroscopically manifested as diffusion, the diffusing process can be evaluated only if flow and temperature fields at the pore scale are known. This is essentially impossible due to the complex cellular morphology of the metal foam, so usually k_d is determined indirectly by matching with macroscopic transport measurements. Thermal dispersion in porous media has been studied by several researchers [7,9,11,17,29], and several empirical models have been proposed based on macroscopic transport measurements. In all these empirical models, the thermal diffusivity is expressed as the product of particle (pore) size, local velocity and dispersion coefficient. Here, the thermal dispersion model developed by Georgiadis and Catton [29] based on stochastic phenomena is adopted, as:

$$k_d = \frac{C_d}{1-\varepsilon}\rho_f C_f d|V| \tag{27}$$

where $C_d = 0.36$ was shown to give the best fit with experimental data [29].

3.3.5. Surface area density $\tilde{a}$ and interstitial heat transfer coefficient h_{sf}

Before carrying out numerical calculations, the surface area density, $\tilde{a}$, and interstitial heat transfer

coefficient, h_{sf}, also need to be determined for the metal foams. The solid–fluid interfacial surface area density based on arrays of parallel cylinders intersecting in three mutually perpendicular directions is [26]:

$$\tilde{a} = \frac{3\pi d_f}{d_p^2} \tag{28}$$

As for the interstitial heat transfer coefficient, h_{sf}, no correlation exists for metal foams. Here, based on the work of Churchill and Chu [30] for natural convection in a bank of staggered cylinders, the following correlation is employed:

$$h_{sf} = \frac{k_f}{d_f}\left(0.36 + \frac{0.518 Ra_d^{1/4}}{\left[1 + (0.559/\mathrm{Pr})^{9/16}\right]^{4/9}}\right) \tag{29}$$

where $Ra_d = g\beta\Delta T d_f^3/(a_f v_f)$.

3.4. Numerical procedure

The combined continuity, momentum, and energy equations are solved numerically with the SIMPLE algorithm [31]. The control-volume formulation utilized in this algorithm ensures the continuity of convective and diffusive fluxes as well as overall momentum and energy conservation. The harmonic mean formulation adopted for the interface diffusion coefficients between two control volumes can handle abrupt changes in these coefficients. Selected calculations show that the mesh size required for sufficient numerical accuracy depend mainly on the Rayleigh and Darcy numbers. For all cases studied, it is found that a uniform grid of 65×55, in axial and radial directions respectively, can ensure the mesh-independence of the solution. The governing equations were solved by using the ADI numerical scheme. The iteration is terminated when changes in target variables (u, v, T_s and T_f) are less than 10^{-5} between successive iterations.

4. Results and discussion

4.1. Effect of Darcy number, Da

Fig. 5 shows the variation of effective thermal conductivity k_e with the Darcy number Da for sample 3 (Table 1), at a fixed Rayleigh number, $Ra = 48{,}000$. When Da is less than the critical value 4×10^{-3}, k_e remains constant. This implies that no fluid motion (natural convection) occurs and heat is transferred by pure conduction, a typical feature of the Rayleigh–Benard problem. When the Darcy number exceeds the critical value 4×10^{-3}, the value of k_e sharply increases (Fig. 5), as a result of natural convection. Here, another parameter, the medium Rayleigh number, is introduced

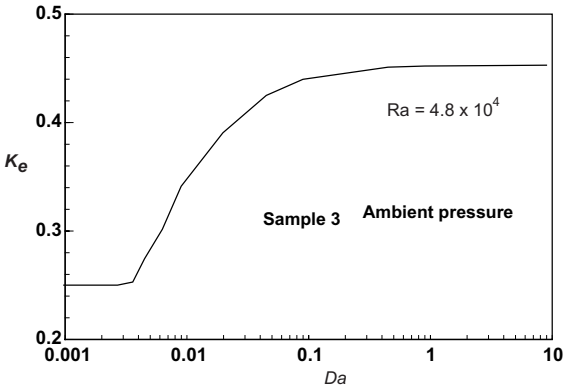

Fig. 5. Effect of Darcy number on natural convection (sample 3).

as $Ra_m = RaDa\ k_f/k_m$, which can be considered as the combined effect of buoyancy force and permeability. Here k_m is the saturated medium thermal conductivity, its value can be predicted by Eqs. (23) and (24) as $k_m = k_{se}$ if the conduction of air is neglected. The corresponding critical medium Rayleigh number, Ra_m^c, is about 20 for the onset of natural convection. For the Benard-type natural convection problem between two infinite horizontal plates, the onset of natural convection occurs at $Ra_m \approx 40$ [27,29]. Since the case studied here is natural convection confined inside a cylinder with $r_0/H \approx 2$–3, the boundary condition has a direct effect on the onset of natural convection. As the Darcy number Da exceeds the critical value, the effective conductivity k_e drastically increases from 0.25 W/mK, and then approaches asymptotically 0.45 W/mK when $Da > 0.1$. Given that $Da = K/H^2$, increasing Da is equivalent to increasing the permeability for a fixed height, H. Therefore, the maximum of k_e, 0.45 W/mK, should be identical to the value obtained from natural convection in the single fluid medium with same equivalent thermal conductivity as the metal foam studied.

4.2. Effect of Rayleigh number, Ra

In a number of studies [3,9,32], the numerical and experimental results were correlated with the porous Rayleigh number Ra_m as follows:

$$Nu_m = \frac{q}{\Delta T}\frac{H}{k_m} = \frac{k_e}{k_m} = f(Ra_m) = CRa_m^n \tag{30}$$

Note that Nu_m is based on the medium thermal conductivity, k_m. This correlation indicates that Nusselt number is only dependent on Ra_m. However, from Eq. (11), the parameters Ra and Da cannot be simply integrated as one independent parameter Ra_m. Namely, the effects of porous resistance and buoyancy force (Ra) on heat transfer are somewhat different, and

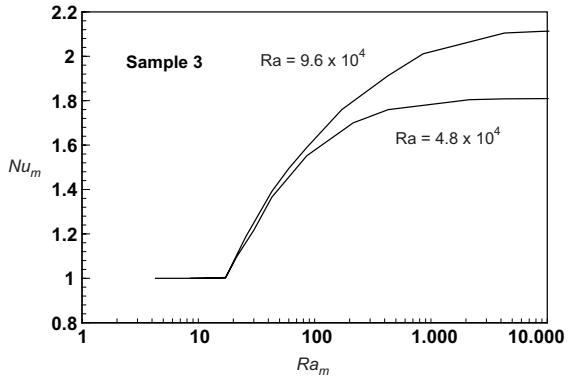

Fig. 6. Effect of Rayleigh number on natural convection (sample 3).

therefore the effect of Ra cannot be simply ascertained by using a combined parameter Ra_m. Fig. 6 presents Nu_m as a function of Ra_m for two different Rayleigh numbers. It is seen that Nu_m is (approximately) independent of Ra only when $Ra_m < 100$. Beyond this range, for a given Ra_m, the value of Nu_m increases with increasing Rayleigh number, implying that the enhancing effect due to stronger buoyancy outstrips the suppressing effect of diminishing permeability. A similar conclusion on the Ra effect was reached by Kaviany [4] who studied non-Darcian effects on natural convection in porous media confined between horizontal cylinders. For high porosity, open-celled metal foams, the buoyancy permeability and the corresponding Darcy number could be much higher: it is therefore most likely that Ra_m lies beyond the range where Nu_m is only dependent on the combined effect of Ra_m.

4.3. Velocity fields, temperature distributions and local heat transfer

The effective thermal conductivities of FeCrAlY foams have been measured for different relative densities and cell sizes at various temperatures between room temperature and 800 K [24]. Numerical calculations based on the natural convection model developed here have been conducted for the same samples (Table 1). As thermal radiation is not considered in the present mathematical formulations, only the effective thermal conductivity measured at the lowest temperature for each sample will be used to compare with numerical predictions. The Rayleigh number Ra in the measurements is approximately 5×10^4 for all samples. From Fig. 5, the Darcy number has almost no effect on overall heat transfer when Da exceeds 0.1. In view of the high porosity and inter-connected open cells of metal foams, it is assumed here that the Da number based on the buoyancy permeability lies beyond this range, i.e., $Da > 0.1$. This implies that the foam structure imposes little restriction on natural convection flow at the global scale. Therefore, the Darcy term in Eqs. (12) and (13) is neglected in all calculations. Results for sample 2 with 30 ppi and 10% relative density are presented below; similar results are obtained for the rest of the samples.

4.3.1. Velocity field

Fig. 7 depicts the velocity field for sample 2 at $Ra = 5.0 \times 10^4$, where three major counter-rotating rolls (circulation zones) are visible. To have a clearer picture on the velocity field, the stream function ψ is introduced, defined as $\partial\psi/\partial r = ru$, $\partial\psi/\partial x = -rv$. The contour of the stream function is plotted in Fig. 8. The three major rotating rolls are clearly shown in this figure.

4.3.2. Solid and fluid temperature distributions

The contours of temperature distributions in the solid and fluid phases are presented in Figs. 9a and b,

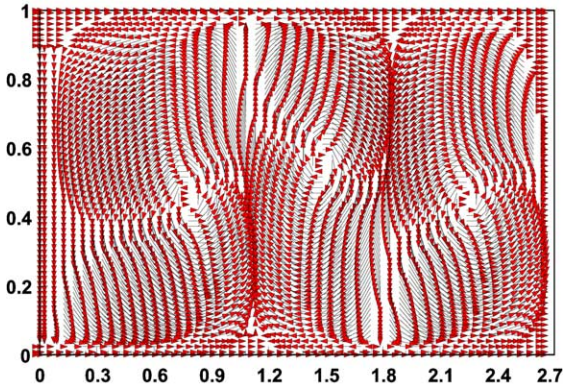

Fig. 7. Velocity profile of natural convection in sample 2 ($Ra = 5 \times 10^4$).

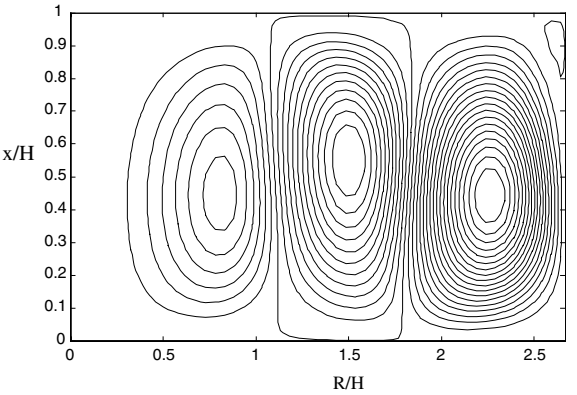

Fig. 8. Contour plot of stream function in sample 2 ($Ra = 5 \times 10^4$).

respectively, for sample 2 at $Ra = 5.0 \times 10^4$. The solid temperature decreases linearly from the bottom surface to top surface, wiggling slightly in the horizontal direction due to natural convection (Fig. 9a). The fluid temperature exhibits much stronger wave distributions (Fig. 9b), owing to the strong counter-rotating rolls shown in Figs. 7 and 8. The fluid temperature distribution is totally different from that of the solid, indicating that the commonly used one-equation energy model based on local thermal equilibrium is not adequate for studying natural convection in metal foams.

To make a clearer examination and comparison, Fig. 10 depicts metal and air temperature distributions at three selected horizontal levels, $X = 0.1$, 0.5, and 0.9 (sample 2, $Ra = 5.0 \times 10^4$). It can be seen that the metal and air temperature lines both resemble sine waves, but the amplitude of air temperature lines is much larger than that of the metal. At the horizontal level of $X = 0.1$ close to the hot surface (bottom surface), metal temperature is higher than air, suggesting that heat is being transferred from former to latter. On the contrary, air temperature is higher than that of metal at the horizontal level of $X = 0.9$ close to the cold plate, resulting heat transfer from air to metal. At the middle level, $X = 0.5$, both situations occur due to the strong three rotating rolls.

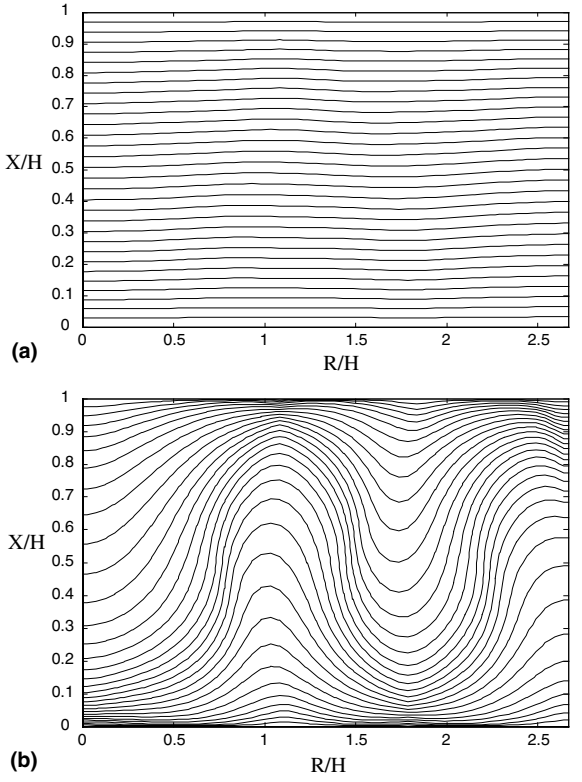

Fig. 9. Temperature contour plot of (a) solid; (b) fluid in sample 2 ($Ra = 5 \times 10^4$).

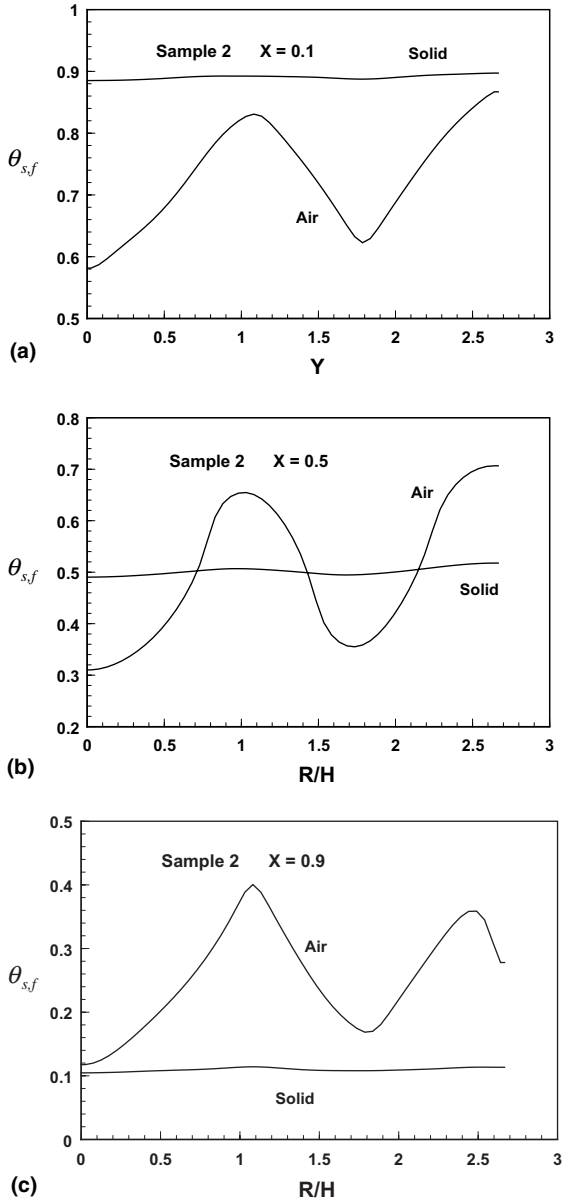

Fig. 10. Non-equilibrium effect on solid and fluid temperature distributions in sample 2 ($Ra = 5 \times 10^4$).

4.3.3. Heat transfer

The local Nusselt number Nu at the bottom and top surfaces of sample 2 is shown in Fig. 11 for $Ra = 5.0 \times 10^4$. Here, the local Nusselt number is defined as:

$$Nu_f = \frac{q}{\Delta T}\frac{H}{k_f} \tag{31}$$

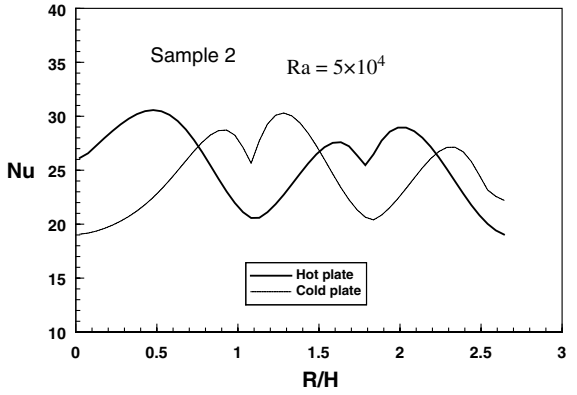

Fig. 11. Distribution of local Nusselt numbers at bottom and top surfaces of sample 2 ($Ra = 5 \times 10^4$).

where

$$q = k_{fe}\left.\frac{\partial T_f}{\partial y}\right|_{y=0} + k_{se}\left.\frac{\partial T_s}{\partial y}\right|_{y=0} \quad (32)$$

Fig. 11 shows that the local Nu distributions are quite different for the top and bottom surfaces, even though their averaged values are identical. Again, this is attributed to the effect of strong rotating rolls of air.

4.4. Comparison with experimental measurements

The comparison of numerical predictions and experimental measurements on room temperature effective thermal conductivity is presented in Fig. 12 for all five FeCrAlY foam samples. Generally, the predictions agree well with experimental data, with a maximum deviation of 28% for sample 2. It is noted that the deviation for two samples with 10% relative density is larger than that of other samples with 5% relative density. For the larger relative density (10%) sample, the natural convection will be enhanced by more high-temperature solid structure presence. The stronger natural convection may result in three-dimensional cellular patterns or eventually chaotic motion, which makes the two-dimension assumption inadequate.

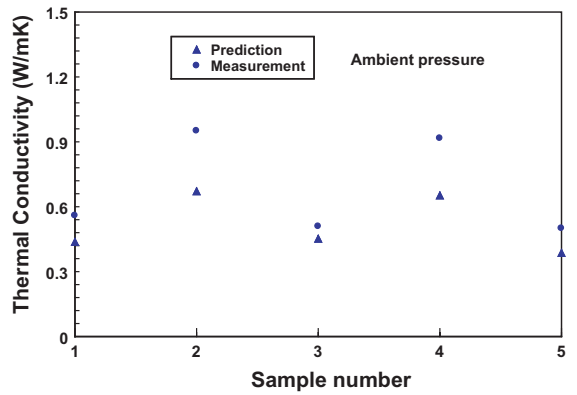

Fig. 12. Comparison between measurements and predictions of effective thermal conductivity for 5 FeCrAlY foam samples at room temperature.

5. Conclusions

Natural convection and its effect on overall heat transfer in highly porous, open-celled cellular FeCrAlY foams have been experimentally and numerically investigated. The following major conclusions can be drawn:

(a) Natural convection is very significant in metal foams due to the high porosity and inter-connected open cells, contributing more than 50% of the effective conductivity at ambient pressure.
(b) The combined parameter, porous medium Rayleigh number Ra_m, cannot characterize natural convection alone when the Darcy number is relatively large, as in the case of high-porosity metal foams.
(c) Numerical calculations show that the non-equilibrium effect, i.e., the temperature difference between solid and fluid phases, cannot be neglected, and hence the commonly used one-equation model is no longer suitable for natural convection in metal foams: the non-equilibrium two-equation energy model should be used.
(d) The predicted effective thermal conductivities of FeCrAlY foams compare favourably with those measured at room temperature with the guarded-hot-plate method.

Acknowledgments

This work is supported by the UK Engineering and Physical Sciences Research Council (EPSRC grant number GR/T24364/01), Brief Award of Brunel University (WAE-DPA301) and Research Grant of China. The authors also wish to thank the assistance of Mr. Ian Stirling, Porvair Plc., for providing test samples.

References

[1] A. Bejan, D. Poulikakos, The non-Darcy regime for vertical boundary layer natural convection in a porous medium, Int. J. Heat Mass Transfer 27 (5) (1984) 717–722.
[2] V. Prasad, F.A. Kulacki, M. Keyhani, Natural convection in porous media, J. Fluid Mech. 150 (1985) 89–119.

[3] V. Prasad, F.A. Kulacki, Natural convection in porous media bounded by short concentric vertical cylinders, J. Heat Transfer 107 (1985) 147–154.
[4] M. Kaviany, Non-Darcian effects on natural convection in porous media confined between horizontal cylinders, Int. J. Heat Mass Transfer 29 (10) (1986) 1513–1519.
[5] C. Beckermann, S. Ramadhyani, R. Viskanta, Natural convection flow and heat transfer between a fluid layer and a porous layer inside a rectangular enclosure, J. Heat Transfer 109 (1987) 363–370.
[6] J.T. Hong, Y. Yamada, C.L. Tien, Effects of non-Darcian and nonuniform porosity on vertical-plate natural convection in porous media, J. Heat Transfer 109 (1987) 356–362.
[7] J.T. Hong, C.L. Tien, Analysis of thermal dispersion effect on vertical-plate natural convection in porous media, Int. J. Heat Mass Transfer 30 (1) (1987) 143–150.
[8] T. Jonsson, I. Catton, Prandtl number dependence of natural convection in porous media, J. Heat Transfer 109 (1987) 371–377.
[9] S.W. Hsiao, P. Cheng, C.K. Chen, Non-uniform porosity and thermal dispersion effects on natural convection about a heated horizontal cylinder in an enclosed porous medium, Int. J. Heat Transfer 35 (12) (1992) 3407–3418.
[10] P. Vadasz, The effect of perfectly conducting side walls on natural convection in porous media, Int. J. Heat Mass Transfer 36 (5) (1993) 1159–1170.
[11] L.E. Howle, J.G. Georgiadis, Natural convection in porous media with anisotropic dispersive thermal conductivity, Int. J. Heat Mass Transfer 37 (7) (1994) 1081–1094.
[12] I. Pop, D. Angirasa, G.P. Peterson, Natural convection in porous media near L-shaped corners, Int. J. Heat Mass Transfer 40 (2) (1997) 485–490.
[13] A. Chakma, E. Choi, A bifurcation study of natural convection in a porous media with internal heat sources: the non-Darcy effects, Int. J. Heat Mass Transfer 41 (2) (1998) 383–392.
[14] L.S. Alves, B. de, R.M. Cotta, J. Pontes, Stability analysis of natural convection in porous cavities through integral transforms, Int. J. Heat Mass Transfer 45 (2002) 1185–1195.
[15] J.T. Hong, C.L. Tien, M. Kaviany, Non-Darcian effects on vertical-plate natural convection in porous media with high porosities, Int. J. Heat Mass Transfer 28 (11) (1985) 2149–2157.
[16] M.S. Phanikumar, R.L. Mahajan, Non-Darcy natural convection in high porosity metal foams, Int. J. Heat Mass Transfer 45 (2002) 3781–3793.
[17] M.L. Hunt, C.L. Tien, Effects of thermal dispersion on forced convection in fibrous media, Int. J. Heat Mass Transfer 31 (1988) 301–309.
[18] J.W. Paek, B.H. Kang, S.Y. Kim, J.M. Hyun, Effective thermal conductivity and permeability of aluminium foam materials 21 (2) (2000) 453–464.
[19] V.V. Calmidi, R.L. Mahajan, Forced convection in high porosity metal foams, J. Heat Transfer 122 (2000) 557–565.
[20] N.D. Ngo, K.K. Tamma, Microscale permeability predictions of porous fibrous media, Int. J. Heat Mass Transfer 44 (2001) 3135–3145.
[21] I.F. Macdonald, M.S. El-Sayed, K. Mow, F.A.L. Dullien, Flow through porous media: The Ergun equation revisited, Indust. Eng. Chem. Fundament. 18 (1979) 199–208.
[22] B.V. Antohe, J.L. Lage, D.C. Price, R.M. Weber, Experimental determination of permeability and inertial coefficients of mechanically compressed aluminium porous matrices, J. Fluids Eng. 119 (1997) 404–412.
[23] J.L. Lage, B.V. Antohe, D.A. Nield, Two types of nonlinear pressure-drop versus flow-rate relation observed for saturated porous media, J. Fluids Eng. 119 (1997) 700–706.
[24] C.Y. Zhao, T.J. Lu, H.P. Hodson, J.D. Jackson, The temperature dependence of effective thermal conductivity of open-celled steel alloy foams, Mater. Sci. Eng.: A 367 (2004) 123–131.
[25] C.Y. Zhao, Thermal transport in cellular metal foams with open cells, PhD thesis, Engineering Department, Cambridge University, June 2003.
[26] C.Y. Zhao, T. Kim, T.J. Lu, H.P. Hodson, Thermal transport in high porosity cellular metal foams, J. Thermophys. Heat Transfer 18 (2004) 309–317.
[27] A. Bejan, Convection Heat Transfer, second ed., Wiley & Sons Inc, New York, 1994.
[28] K. Boomsma, D. Poulikakos, On the effective thermal conductivity of a three-dimensionally structured fluid-saturated metal foam, Int. J. Heat Mass Transfer 44 (2001) 827–836.
[29] J.G. Georgiadis, I. Catton, Dispersion in cellular thermal convection in porous layers, Int. J. Heat Mass Transfer 31 (5) (1988) 1081–1091.
[30] S.W. Churchill, H.H.S. Chu, Correlating equations for laminar and turbulent free convection from a vertical plate, Int. J. Heat Mass Transfer 18 (1975) 1323–1329.
[31] S. Patankar, Numerical Heat Transfer and Fluid Flow, Hemisphere, New York, 1980.
[32] D.J. Close, J.G. Symons, R.F. White, Convective heat transfer in shallow gas-filled porous media: experimental investigation, Int. J. Heat Mass Transfer 28 (12) (1985) 2371–2378.